Bioscience Reports (2020) **40** BSR20193512
https://doi.org/10.1042/BSR20193512

PORTLAND PRESS

Research Article

Estradiol and progesterone affect enzymes but not glucose consumption in a mink uterine cell line (GMMe)

Hayden Holmlund[1], Álvaro Marín-Hernández[2] and Jennifer R. Chase[1]

[1]Northwest Nazarene University, 623 S. University Blvd, Nampa, ID 83686, U.S.A.; [2]Departamento de Bioquímica, Instituto Nacional de Cardiología, Mexico City 14080, México

Correspondence: Jennifer R. Chase (jrchase@nnu.edu)

Cells lining the uterus are responsible for storage and secretion of carbohydrates to support early embryonic development. Histotrophic secretions contain glycogen and glycolytic products such as lactate and pyruvate. Insufficient carbohydrate storage as glycogen has been correlated with infertility in women. While it is clear that changes in estrogen (17-β-estradiol (E_2)) and progesterone (P_4) *in vivo* affect the distribution of glucose in the uterine cells and secretions, the biochemical mechanism(s) by which they affect this crucial allocation is not well understood. Furthermore, in cultured uterine cells, neither E_2 nor P_4 affect glycogen storage without insulin present. We hypothesized that P_4 and E_2 alone affect the activity of glycolytic enzymes, glucose and glycolytic flux to increase glycogen storage (E_2) and catabolism (P_4) and increase pyruvate and lactate levels in culture. We measured the rate of glucose uptake and glycolysis in a mink immortalized epithelial cell line (GMMe) after 24-h exposure to 10 μM P_4 and 10 nM E_2 (pharmacologic levels) at 5 mM glucose and determined the kinetic parameters (V_{max}, K_m) of all enzymes. While the activities of many glycolytic enzymes in GMMe cells were shown to be decreased by E_2 treatment, in contrast, glucose uptake, glycolytic flux and metabolites levels were not affected by the treatments. The cellular rationale for P_4- and E_2-induced decreases in the activity of enzymes may be to prime the system for other regulators such as insulin. *In vivo*, E_2 and P_4 may be necessary but not sufficient signals for uterine cycle carbohydrate allocation.

Introduction

A fertilized human embryo is estimated to have only a 30% chance of implanting in the uterine wall [1]. Failure of implantation is approximately 30–40% for fertilized embryos in cattle, with a lower rate estimated for sheep, which is highly correlated to circulating progesterone (P_4) [2]. It is likely that some of these losses are the result of inadequate P_4 and 17-β-estradiol (E_2)-stimulated nutrient storage by uterine glands and/or failure to mobilize the nutrients toward the uterine lumen as the embryo is rapidly growing until it implants in the uterine wall. Before implantation, lactate and pyruvate are essential for development of mammalian embryos to *at least* the morula stage [3,4]. It is thus essential to assess the cellular mechanisms that regulate the production of these molecules in order to understand how to maximize fertility.

Glandular epithelial cells are responsible for supplying nutrients to the embryo during the first trimester of pregnancy in a process that is coordinated by both P_4 and E_2. In humans, P_4 produced by the corpus luteum promotes the secretory transformation of the endometrial epithelial glands that will, in response to E_2, produce a uterine milk called histotroph containing glucose, lactate, pyruvate and amino acids which support the developing embryo at least until placentation is complete [5,6]. In mustelids, E_2 levels peak before ovulation and rise with P_4 levels, which are highest during peri-implantation [7].

Received: 21 October 2019
Revised: 25 March 2020
Accepted: 26 March 2020

Accepted Manuscript online: 02 April 2020
Version of Record published: 24 April 2020

Bioscience Reports (2020) **40** BSR20193512
https://doi.org/10.1042/BSR20193512

P_4 and E_2 affect glucose metabolism during the uterine cycle *in vivo*. E_2 promotes glycogen storage in mammals *in vivo*, while elevated P_4 promotes catabolism of the stored carbohydrate [8–11]. Glycolysis, too, is highest in estrus, when E_2 is elevated in bovine [12] and rat uterus [13]. In rats, all glycolytic enzymes increase their activity in response to estrogen [14], while P_4 counters the stimulatory effects of E_2 on pyruvate kinase (PYK; E.C. 2.7.1.40) and hexokinase (HK; E.C. 2.7.1.1) activities [15,16]. However, in sheep the activities of lactate dehydrogenase (LDH, E.C. 1.1.1.27) and glucose-6-phosphate dehydrogenase (G6PDH; E.C. 1.1.1.49) did not change significantly during the estrus cycle [17,18]. Enzyme activities have not been reported for specific endometrial cell types under physiological conditions and kinetic parameters have not been thoroughly studied in endometrial tissue of any organism.

The American mink (*Neovison vison*) is a significant model organism in the study of uterine carbohydrate metabolism in reproduction. Mink exhibit an obligatory embryonic diapause, often having blastocysts suspended 50–60 days *post-coitum*. P_4 stimulates uterine glycogen catabolism in the mink endometrium, whereas E_2 promotes glycogen accumulation *in vivo* [19,20] and in cultured cells in the presence of insulin. The mechanisms by which E_2 and P_4 directly affect glycolysis and its enzymes in uteri have not been determined in mink and other mammals because of the confounding effect of hormones such as insulin.

Mink immortalized endometrial cells (GMMe) [21] provide an ideal model system to study hormonal regulation of glycolysis in the uterus, not only because carbohydrate metabolism has already been studied in mink uterus and in GMMe, but also because they are one of the only immortalized endometrial cell lines that are commercially available. They respond to E_2 and P_4 [22,23] and express estrogen receptor Type 1 [22]. They also represent a source of mink enzymes, for which few K_ms have been determined under any conditions [24]. This also isolates the behavior of epithelial cells where most of the glycogen is stored [19,20], compared with the *in vivo* studies which work with homogenized uterine tissue containing both stromal and epithelial tissues.

P_4 and E_2 affect enzymes involved in glucose and glycogen metabolism in the mink endometrium. Glycogen phosphorylase and HK-1 levels are highest during estrus and diapause, glucose-6-phosphatase levels are highest during diapause, while glycogen synthase levels are undetectable after estrus [20]. However, hormonal regulation has not been studied for mink glycolytic enzymes other than HK and no kinetic studies have been done in GMMe. Measuring glycolytic enzyme kinetics will help determine *how* P_4 and E_2 affect carbohydrate allocation in mink uterine cells.

Though P_4 and E_2 are essential for changing carbohydrate usage and enzymes in mink endometrial tissue, *in vitro* it has been shown that E_2, at least, must act in coordination with other hormones (primarily insulin) to affect glycogen levels. In GMMe, E_2 enhances insulin's stimulatory effect on glycogen storage, while E_2 alone has no effect on glycogen levels [22]. Thus, any changes to glycolytic enzymes by P_4 and E_2 alone may not affect carbohydrate usage directly, but rather play a larger role in priming the system for hormonal regulation by insulin.

The enzyme mRNA level is often used as a proxy for levels of enzymes, but a quantitative estimation of their maximum velocities requires direct measurement of their activity. This is the first study of glycolysis and glycolytic enzyme kinetics in immortalized endometrial cells. We measured the rate of glycolysis in GMMe cells after 24 h of exposure to 10 μM P_4 and 10 nM E_2 at 5 mM glucose and the kineticparameters (V_{max}, K_m) of glycolytic enzymes, phosphoglucomutase (PGM; E.C. 5.4.2.2) and G6PDH spectrophotometrically with coupled assays. The activity of several glycolytic enzyme activities in GMMe cells were decreased by E_2 treatment, whereas their K_ms were increased by P_4 treatment though glucose uptake, glycolytic flux and metabolite values were unchanged by the treatments.

Methods

$NADP^+$ and NAD^+ were purchased from Research Products International. All other chemicals and enzymes were purchased from Sigma–Aldrich. The concentrations in stock solutions of substrates were calibrated spectrophotometrically by enzymatic assays, monitoring changes in NAD(P)H using $\varepsilon = 6.22\ mM^{-1}.cm^{-1}$.

Cell culture

GMMe (ATCC® CRL-2674™) cells were used between passages 4 and 19 and cultured in growth media (DMEM/F-12, 5% FBS, 1% pen/strep, 16 mM glucose, no Phenol Red; #DFL-14, Caisson Labs, Smithfield, UT) in humidified air: 95%, CO_2: 5%, 37°C in 75- or 175-cm^3 culture flasks. Medium was refreshed every ∼3 days and replaced with sterile medium. Cells were passaged when ∼90% confluent at a subcultivation ratio of 1:2 to 1:6. For the last 24 h, the medium was replaced with DMEM/F-12 (5 mM glucose) every 12 h, with 10 nM E_2, 10 μM P_4 or dimethyl sulfoxide (DMSO; control) vehicle. These hormone levels were shown to be the minimum necessary to affect insulin receptor and, with insulin, glycogen levels in GMMe cells [22,23]. These levels were several orders of magnitude smaller than what was measured *in vivo* in mink [25]. E2 (E2758, Sigma–Aldrich) and P_4 (P783; Sigma–Aldrich)

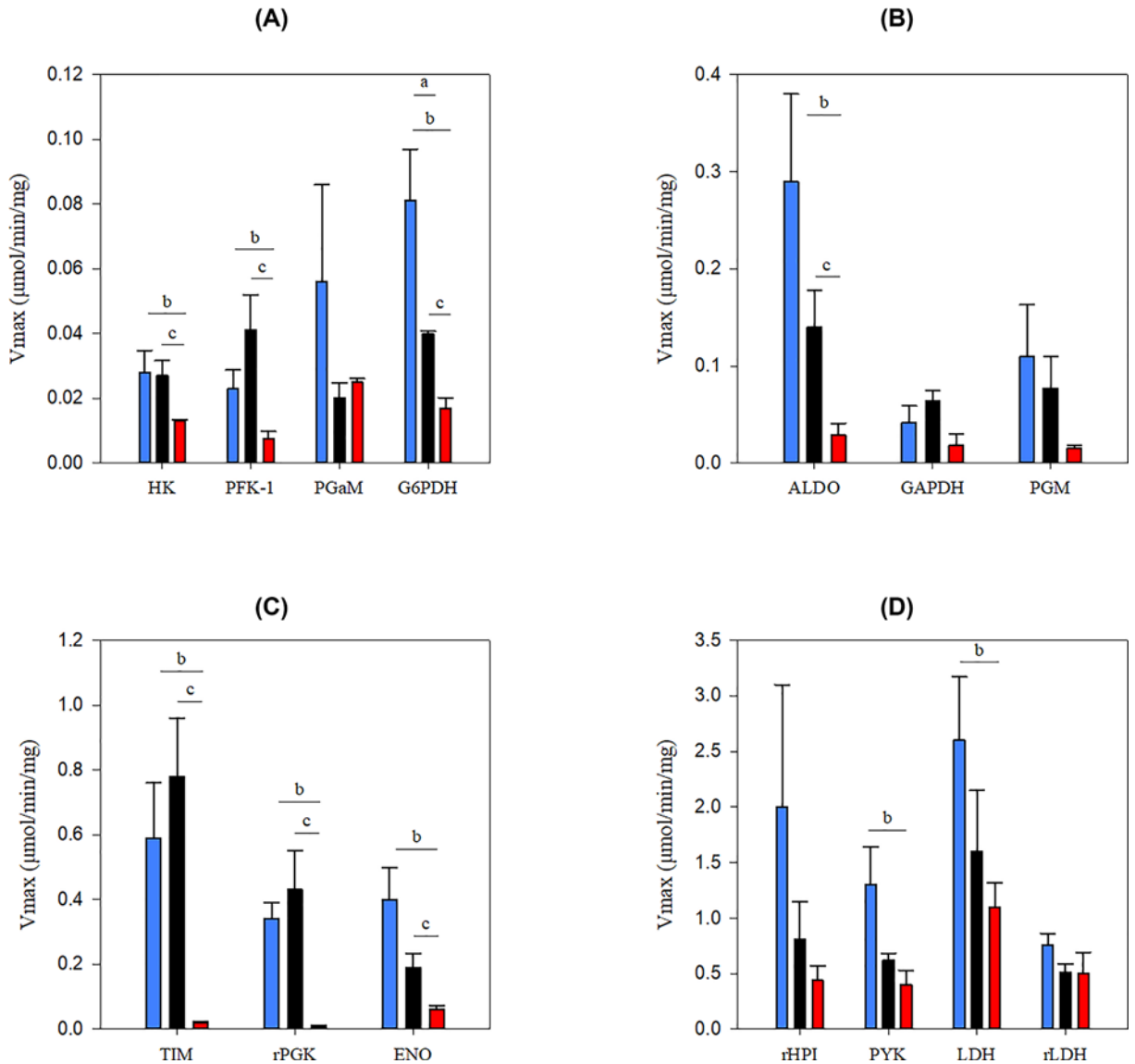

Figure 1. Maximum velocities of glycolytic enzymes

Average maximum velocities shown (±SEM of three independent preparations assayed) with 2% Triton X-100. (a vs. control, b vs. E_2, c P_4 vs E_2, $P<0.05$). Control (blue), P_4 (black), E_2 (red). **(A–D)** grouped by increasing V_{max}.

were dissolved in 100% DMSO (Sigma–Aldrich, Hybri-Max™) to make stock solutions (50 µM E_2 and 100 mM P_4). Medium glucose at 5 mM was used [22], which is similar to blood glucose in mink during the breeding season (~5.3 mM) [26,27].

Before harvesting, the cell layer was washed with 3–6 ml of PBS to remove all media. The cells were incubated with 0.25% (w/v) trypsin and 0.53 mM EDTA solution (3–6 ml) for <10 min to dislodge. The cells from this medium, along with one wash of the flask with 5 ml PBS, were pelleted at 2000×***g*** for 5 min, resuspended in PBS to wash and again pelleted/resuspended one to two times. The supernatant was removed, and the cells were resuspended in Krebs–Ringer. This cell suspension was used for determination of maximum velocity in total cells. Harvested cell suspensions were assayed for total protein content using a bicinchoninic acid (BCA) assay [28] and for cell number using a cell counter (Countess II, Life Technologies, Thermo Fisher).

To prepare cytosol-enriched fraction for determination of K_m values, cells were resuspended in enzyme extract buffer (1 ml of 25 mM Tris/HCl, pH 7.6, plus 5 mM DTT, 1 mM EDTA and 1 mM PMSF). The cellular suspension was frozen in liquid N_2, then thawed at 37°C for four cycles. The cellular lysates were centrifuged at 14000 rpm for 20

Bioscience Reports (2020) **40** BSR20193512
https://doi.org/10.1042/BSR20193512

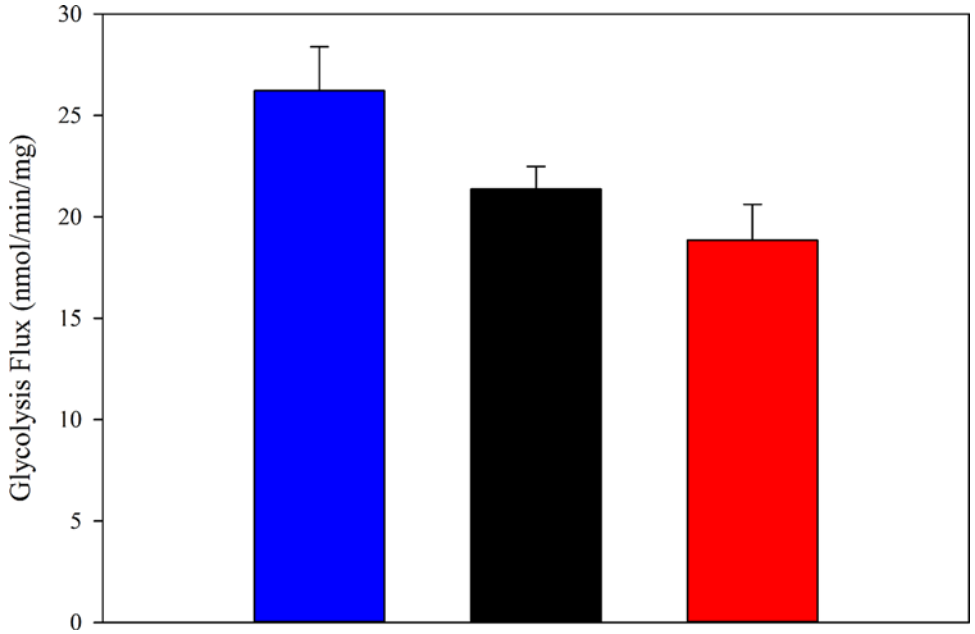

Figure 2. Glycolytic flux

Geometric mean of lactate production in 20 min at 5 mM glucose (±SD, n=4 for control and P_4; n=5 for E_2). Control (blue), P_4 (black) and E_2 (red). n is the number of independent cell batches assayed.

min and 4°C. Afterward, the supernatant (i.e., the cytosolic-enriched fractions) was collected and mixed with glycerol (10%, v/v, final concentration). The protein content was determined by the BCA assay. The material was aliquoted (<1 ml) and stored at −70°C until use.

Glucose uptake

Glucose uptake by GMMe cells was measured using UptakeGlo Assay (Promega, U.S.A.). Briefly, GMMe cells were seeded (20000 cells/well) in triplicate for each independent cell batch assayed, in a 96-well plate and provided high-glucose medium. After 24 h, the medium was replaced with treatment medium (DMEM/F12, 5 mM glucose, with 10 nM E_2, 10 μM P_4, or DMSO vehicle) which was replaced after 12 h. PBS-washed cells were incubated for 10 min in glucose-deprived medium supplemented with 1 mmol/l 2-Deoxy-D-Glucose. Afterward, cells were lysed and the accumulation of 2-deoxy-glucose 6-phosphate (G6P) was detected using G6PDH and luciferase, which uses the produced NADPH as a substrate. Glucose uptake (nmol/mg/min) was calculated from the time of uptake, the average protein content of matched wells and the amount of 2-deoxy-G6P accumulated. A standard curve of 2DG6P was used to calculate the amount of 2-deoxy-G6P accumulated.

Enzyme assays

Glycolytic enzyme activities and affinity constants were determined for the forward (glycolytic) and reverse (gluconeogenic) reactions. Kinetic parameters (V_{max}, K_m) were determined at 37°C following the $NAD(P)^+$ reduction or nicotinamide adenine dinucleotide phosphate (NADP(H)) oxidation at 340 nm in a HP8453 spectrophotometer (Agilent, Santa Clara, CA) with an eight-cell carrier. All reactions were started by adding the specific substrates. When the specific substrate was omitted from the assay mixture, enzyme activity was absent. In all assays, control experiments were carried out to establish the linearity range of enzyme activities regarding protein added. Initial rates were calculated only the linear part of activity curve using ChemStation software (Agilent, Santa Clara, CA). All assays were carried out in KME buffer (100 mM KCl, 50 mM MOPS, 0.5 mM EGTA, pH 7.0) with the exception of LDH assay in reverse reaction, for which the assay buffer contained 0.4 M hydrazine/0.5 M glycine, pH 9.

V_{max} values were measured in cell suspension by lysing the cells in 0.02% Triton X-100 to obtain the corresponding V_{max} total cellular protein units and know the amount of total active enzyme present in the cells. In order to correctly estimate the V_{max}, the reactions were carried out at saturated concentrations of substrates (at least ten-times K_m). All enzyme activities were measured within 3 h after the cells were harvested.

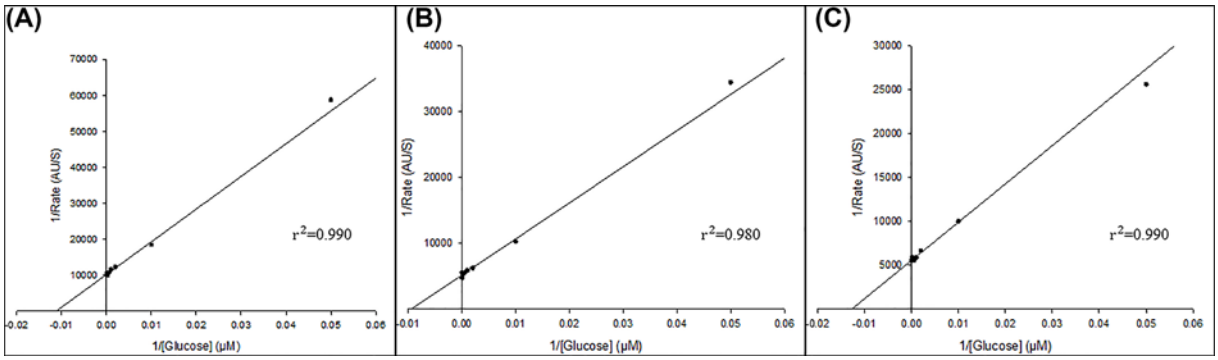

Figure 3. HK Lineweaver–Burk plots

Initial rates measured in GMMe cytosolic enzyme extract (n=1, 5 mM Glucose) for control (**A**), 10 μM P_4 (**B**) and 10 nM E_2 (**C**).

The K_m values were determined in cytosol-enriched fractions by varying the substrate concentrations, as is indicated for each enzyme assay, to ensure that they varied from $<K_m$ to approximately saturation for each enzyme.

The HK activity assay was carried out in the presence of 10 U G6PDH, 500 μM $NADP^+$, 15 mM $MgCl_2$, 150–300 μg of cell protein and variable adenosine triphosphate (ATP; 0.2–10 mM at constant 3 mM glucose) or glucose (0.02–3 mM at constant 10 mM ATP) to determine K_m values for ATP and glucose, respectively; the reaction was started by adding glucose. When HK V_{max} was determined, the ATP and glucose concentrations were 10 and 3 mM, respectively. The reaction was linear for approximately 500–2000 s.

The PGM activity assay for the reverse reaction (glucose 1-phosphate (G1P) → G6P) was carried out in the presence of 10 U G6PDH, 500 μM $NADP^+$, 2 mM $MgCl_2$, 2 μM G1, 6BP and 150–300 μg of cell protein; the reaction was started by adding G1P (0.01–10 mM) to determine K_m value for G1P. When PGM V_{max} was determined, the G1P concentration was 10 mM. The reaction was linear for approximately 500–2000 s.

The G6PDH activity assay was carried out in the presence of 150–300 μg of cell protein, and variable $NADP^+$ (10–700 μM at constant 400 μM G6P) or G6P (1–400 μM at constant 700 μM $NADP^+$) to determine K_m values for $NADP^+$ and G6P, respectively; the reaction was started by adding G6P. When G6PDH V_{max} was determined, the $NADP^+$ and G6P concentrations were 500 and 100 μM, respectively. The reaction was linear for approximately 500–2000 s.

The phosphohexose isomerase (HPI; E.C. 5.3.1.9) activity assay for reverse reaction (fructose 6-phosphate (F6P) → G6P) included 10 U G6PDH, 500 μM $NADP^+$ and 15–30 μg of cell protein; the reaction was started by adding F6P (0.01–2 mM) to determine K_m value for F6P. When HPI V_{max} was determined, the F6P concentration was 2 mM. The reaction was linear for approximately 50–500 s.

The phosphofructokinase type I (PFK-1; E.C. 2.7.1.11) V_{max} assay used 10 U aldolase (ALDO; E.C. 4.1.2.13), 10 U α-glycerophosphate dehydrogenase, 10 U triosephosphate isomerase (TIM; E.C. 5.3.1.1), 5 mM $MgCl_2$, 150 μM NADH, 150–300 μg of cell protein and ATP (700 μM at constant 20 mM F6P); the reaction was started by adding F6P. The F6P and ATP concentrations were 20 mM and 700 μM, respectively. The reaction was linear for approximately 500–2000 s.

The ALDO activity assay used 10 U α-glycerophosphate dehydrogenase, 10 U TIM, 150 μM NADH and 60–120 μg of cell protein; the reaction was started by adding fructose 1,6-bisphosphate (F1,6BP; 0.5–300 μM) to determine K_m value for F1,6BP. When ALDO V_{max} was determined, the F1,6BP concentration was 300 μM. The reaction was linear for approximately 500–2000 s.

The TIM activity assay for forward reaction (TIM*f*, dihydroxyacetone phosphate (DHAP) → glyceraldehyde 3-phosphate (G3P)) used 10 U of glyceraldehyde-3-phosphate dehydrogenase (GAPDH), 1 mM NAD^+, 10 mM arsenate (AsO_4), 5 mM cysteine and 15–30 μg of cell protein; the reaction was started by adding DHAP (0.5–30 mM) to determine K_m value for DHAP. When TIM V_{max} forward was determined, the DHAP concentration was 30 mM. The reaction was linear for approximately 50–500 s.

The TIM activity assay for reverse reaction (TIM*r*, G3P → DHAP) used 150 μM NADH, 2.5 mM EDTA, 10 U α-glycerophosphate dehydrogenase and 5–10 μg of cell protein; the reaction was started by adding G3P (0.1–4.5 mM) to determine K_m value for G3P. The reaction was linear for approximately 50–500 s.

The phosphoglycerate kinase (PGK; E.C. 5.4.2.1) activity assay for reverse reaction (PGKr, 3-phosphoglycerate (3PG) → 1,3-bisphosphoglycerate (1,3BPG)) used 10 U GAPDH, 10 mM ATP, 15 mM $MgCl_2$, 150 μM NADH and

Bioscience Reports (2020) **40** BSR20193512
https://doi.org/10.1042/BSR20193512

150–300 μg of cell protein; the reaction was started by adding 3PG (0.5–10 mM) to determine K_m value for 3PG. When PGK V_{max} reverse was determined, the 3PG concentration was 10 mM. The reaction was linear for approximately 500–2000 s.

The phosphoglycerate mutase (PGaM; E.C. 2.7.2.3) activity assay used 10 U enolase (ENO; E.C. 4.2.1.11, 10 U PYK, 10 U LDH, 1 mM adenosine diphosphate (ADP), 5 mM $MgCl_2$, 150 μM NADH and 150–300 μg of cell protein; the reaction was started by adding 3PG (0.001–3 mM) to determine K_m value for 3PG. When PGaM V_{max} was determined, the 3PG concentration was 3 mM. The reaction was linear for approximately 500–2000 s.

The ENO activity assay was performed using 10 U PYK, 10 U LDH, 1 mM ADP, 5 mM $MgCl_2$, 150 μM NADH and 60–120 μg of cell protein; the reaction was started by adding 2-phosphoglycerate (2PG; 1–200 μM) to determine K_m value for 2PG. When ENO V_{max} was determined, the 2PG concentration was 200 μM. The reaction was linear for approximately 500–2000 s.

The PYK activity assay used 10 U LDH, 5 mM $MgCl_2$, 150 μM NADH, 7.5–15 μg of cell protein and variable ADP (0.1–1 mM at constant 600 μM PEP) or PEP (10–600 μM at constant 1 mM ADP) to determine K_m values for ADP and PEP; the reaction was started by adding PEP. When PYK V_{max} was determined, the ADP and PEP concentrations were 1 mM and 600 μM, respectively. The reaction was linear for approximately 50–500 s.

The LDH activity assay for forward reaction (LDH*f*, pyruvate → lactate) used 7.5–15 μg of cell protein and variable NADH (0.5–150 μM at constant 300 μM pyruvate) or pyruvate (10–300 μM at constant 150 μM NADH) to determine K_m values for NADH and pyruvate; the reaction was started by adding pyruvate. When LDH V_{max} forward was determined, the NADH and pyruvate concentrations were 150 and 300 μM, respectively. The reaction was linear for approximately 50–500 s.

The LDH activity assay for reverse reaction (LDH*r*, lactate → pyruvate) was performed with 15–30 μg of cell protein and variable NAD^+ (10–500 μM at constant 30 mM lactate) or lactate (0.5–30 mM at constant 150 μM NAD^+) to determine K_m values for NAD^+ and lactate; the reaction was started by adding lactate. When LDH V_{max} reverse was determined, the NAD^+ and lactate concentrations were 500 μM and 30 mM, respectively. The reaction was linear for approximately 50–500 s.

Kinetic curves were fitted to the Michaelis–Menten equation using SigmaPlot 12.0 (Systat, San Jose, CA). Lineweaver–Burk plots were used to determine how many isoforms of HK, PGM, ALDO, ENO and PYK were present in GMMe cells.

Glycolytic flux

Glycolytic flux was measured in two ways, by fluorescent measurement of acidification and by quantifying the production of lactate. The pH-Xtra Glycolysis Assay kit (#PH-200-4, Agilent, Santa Clara) was used to determine acidification rate. Briefly, GMMe cells from three distinct cell batches were seeded in triplicate in 96-well plates (100000 cells/well) and grown overnight in high-glucose medium. After 24 h, the medium was replaced with treatment medium (in triplicate, with 10 nM E_2, 10 μM P_4, or DMSO vehicle) which was replaced after 12 h. Each well was washed twice in provided respiration buffer then 90 μl of respiration buffer was added to each well (100 μl to control wells). To each experimental well, 10 μl of 'pH-xtra reagent' (fluorescent probe) was added. The plate was read immediately at 37°C in a BioTek H1M plate reader and the change in fluorescent lifetime from 100 to 300 μs delay and a 30-μs read window (excitation 360 nm, emission 620 nm). The emission lifetime (μs/h) values were corrected based on the signal control wells then scaled to $[H^+]$ by Agilent's 'Data Visualization tool'. The protons produced per hour per milligram of protein was calculated using the protein concentration (BCA assay) in matched wells.

For direct quantification of lactate production, cells (∼1 mg/ml in Krebs–Ringer buffer) were shaken in a water incubator (150 rpm) at 37°C in glass scintillation vials. After 10 min, a 100-μl sample was removed and vortexed with ice-cold PCA/EDTA (final: 3% PCA/1 mM EDTA). Glucose was added to a final concentration of 5 mM and the cells shaken for an additional 20 min. Cells (900 μl) were immediately mixed with PCA/EDTA (final concentration 3% PCA/1 mM EDTA) to stop all metabolism [29].

Universal pH indicator (Fisher) was added (10–25 μl) to each sample. Samples were neutralized with 3 M KOH/0.1 M Tris and left on ice for 45 min to overnight. Protein precipitate was pelleted at 14000 rpm for 40 min. The supernatant was stored at −20°C until it was assayed [29].

Total lactate before and after the 20 min was determined by standard coupled assays with 25 U LDH (from Rabbit muscle, Roche) in 0.4 M hydrazine/0.5 M glycine, pH 9 buffer with 1 mM NAD^+ as substrate. The net change in absorbance at 340 nm was measured in a BioTek Synergy H1M in 96-well polystyrene plates with the pathlength-corrected for each well in duplicate. The rate of lactate produced was calculated as the difference between the initial and final samples, standardized to the amount of protein per minute. The glycolytic flux was calculated for

Table 1 K_m values determined in cytosol-enriched fraction from GMMe cells (±SD) and from the BRENDA enzyme database (www.brenda-enzyme.org) for *Rattus norvegicus*

Enzyme		Control	10 μM P_4	10 nM E_2	*R. norvegicus* range
HK	Km_{gluc}	91 ± 17	110 ± 42	63 ± 15	25–150
	Km_{ATP}	830 ± 250	540 ± 180	ND	400–700
G6PDH	Km_{G6P}	45.5 ± 0.6	22 ± 9.0[1]	37 ± 19	2–70
	Km_{NADP}	40 ± 15	5.8 ± 3.3[1,2]	68 ± 37 (4)	0.3–23
PGM	Km_{G1P}	26 ± 15	52 ± 9.0[1]	1200 ± 350[2,3]	Na
HPI	Km_{F6P}	61 ± 18	200 ± 22 (2)[1,2]	88 ± 43	Na
ALDO	$Km_{F1,6bP}$	11 ± 1.7	16 ± 15	ND	8.9
TIM	Km_{G3P}	380 ± 290	ND	ND	Na
	Km_{DHAP}	2200 ± 1800	ND	ND	Na
PGK	Km_{3PG}	1700 ± 510	ND	ND	1400–1700
PGaM	Km_{3PG}	5.9 (1)	20 (1)	ND	Na
ENO	Km_{2PG}	4.9 ± 1.2	27 ± 6.7[1]	11 ± 2.1[2,3]	36–140
PYK	Km_{PEP}	230 ± 19	210 ± 290	ND	180–960
	Km_{ADP}	230 ± 110	260 ± 120	ND	80–1500
LDH	Km_{Pyr}	65(2)	140 ± 18[1]	92 ± 27[3]	Na
	Km_{NADH}	3.4 (2)	15 ± 17	ND	Na
	Km_{Lac}	6500 ± 1200	5700 ± 3200	ND	1800
	Km_{NAD}	170 ± 39	89 ± 50	ND	Na

For all GMMe parameters, n=3 unless noted in parentheses (1 vs. control, 2 vs. E_2, 3 P_4 vs E_2, P<0.05). n is the number of independent cell batches assayed. K_m values in μM. Abbreviations: Na, no data in BRENDA database; ND, not determined.

each condition as the geometric mean and standard deviation of the log of the distribution for three independent cell batches assayed.

Steady-state phosphoenolpyruvate (PEP) and pyruvate concentrations were measured in the same supernatant using coupled assays in HEPES buffer (50 mM HEPES, 1 mM EGTA, pH 7.4) with 0.45 mM NADH, 2.5 mM inorganic phosphate (Pi), 1 mM ADP and 10 mM $MgCl_2$. The reaction was started by adding 10 U PYK that quantified the amount of PEP and after LDH (2.5 U) that consumed the pyruvate. The concentrations were determined and changes in absorbance at 340 nm were measured, in duplicate, in a BioTek Synergy H1M in 96-well polystyrene plates with the pathlength corrected for each well. The intracellular concentrations were calculated from the amount of protein (considering that 2.28 μl/1.8 mg of cellular protein [30]).

Statistical analysis

t tests were used for non-paired samples, with <0.05 being the criterion for significance. For metabolites and fluxes, *t* tests used the log values.

Results

Enzyme kinetics

E_2 treatment significantly decreased (17–60%) the maximum velocities of HK, G6PDH, PFK-1, ALDO, TIM, PGK and ENO relative to both P_4 treatment and control (Figure 1A–C). Additionally, the activities of PYK and LDH were significantly lower (27–42%) with E_2 treatment than control (Figure 1D). Only G6PDH was lower (50%) with P_4 treatment than control (Figure 1A). For all conditions, HK and PFK-1 had, on an average, the lowest maximum velocities, although exposure to E_2 did lower the maximum velocities of TIM and PGK to similar levels (<20 nmol/min/mg cell protein) (Figure 1A,C). Such decreases in glycolytic enzyme levels might modify the concentrations of glycolytic metabolites and glycolytic flux, if these enzymes exert control on glycolytic flux.

The Michaelis constants ($K_m s$) were also measured to provide a complete kinetic data set for mammalian glycolysis (Supplementary Figure S1A–M). P_4 treatment significantly increased (2–5.5 times) the $K_m s$ of PGM, ENO and LDH (Km_{G1P}, Km_{2PG} and Km_{Pyr}), but decreased (14–48%) the $K_m s$ of G6PDH (Km_{G6P} and Km_{NADP}) in comparison with control (Table 1). E_2 treatment significantly increased (1.4–46 times) Km_{G1P}, Km_{2PG} and Km_{Pyr} (Table 1). For E_2 treatment, Km_{2PG} and Km_{Pyr} were significantly lower (37–66%) than P_4 treatment, while Km_{G1P} was 23-times higher (Table 1).

Bioscience Reports (2020) **40** BSR20193512
https://doi.org/10.1042/BSR20193512

Multiple isoforms have been identified in mammalian uterine tissue for PGM, ALDO, PYK, ENO and HK. We did not observe more than one isoform for each of these enzymes in any condition because there was no significant change in the slope of the Lineweaver–Burk plots of any enzyme ($r^2 \geq 0.8$) (Figure 3, Supplementary Figure S2). Although only one isoform of each enzyme was detected, the changes observed in the kinetic parameters might be altered by post-translational modifications (phosphorylation or acetylation), modifying enzyme expression levels or by completely changing which isoform is expressed.

Glucose uptake and glycolytic flux

Fluorescent determination of relative proton production from glycolysis showed no difference between the treatments with vehicle, P_4 or E_2 (7.3 $\pm$ 0.9, 6.6 $\pm$ 1 and 6.2 $\pm$ 1.4 pmol/min/mg protein, respectively). Lactate concentration increased linearly over at least 20 min, consistent with the system being in steady state. For control, the lactate levels in GMMe during the 20-min incubation in 5 mM glucose increased from 0.32 to 0.63 mM. The glycolytic flux did not significantly change under the exposure to P_4 or E_2 (Figure 2). The calculated rate of 26 $\pm$ 2 nmol/min/mg of cells (control) is comparable with that of HeLa cells (21 nmol/min/mg cells, [10]). The lactate concentration is somewhat lower ($\sim$1 mM) than that observed in HeLa cells at 5 mM glucose (27 mM, [10]). Glucose uptake was unchanged by E_2 and P_4 treatment (control: 8.0 $\pm$ 1.4; E_2: 7.6 $\pm$ 1.1; P_4: 9.5 $\pm$ 1.6 nmol/min/mg protein). Considering that each glucose molecule gives two lactate molecules, these values suggest that the majority of the glucose use in the cell is for glycolysis under all three conditions.

Also, pyruvate and PEP levels were unchanged by hormone treatment (PEP: 5.8 $\pm$ 1.6, 5.8 $\pm$ 2.2, 8.45 $\pm$ 3.3 mM, n=5; pyruvate: 6.1 $\pm$ 2.0, 7.5 $\pm$ 2.9, 11.5 $\pm$ 1.6 mM, n=5) for control, E_2 and P_4, respectively. These concentrations are similar to levels observed in AS-30D rat cells [31]. Because they are more than ten-times higher than the $K_m s$ as substrates for PYK and LDH, respectively, those enzymes remain essentially saturated with PEP or pyruvate under all three conditions. However, to determine if, under physiological conditions, the enzymes are at V_{max}, it would be necessary to determine the concentration of the other substrates: ADP (PYK) and NADH (LDH).

Alterations in PGM kinetics by hormones may affect glycogen metabolism, as E_2 and P_4 treatment decrease the V_{max} and increase K_m to G1P relative to control. At cellular G1P concentrations (4.5 mM, unchanged by hormones), PGM activity was reduced by 31% for P_4 treatment but 89% for E_2 treatment, suggesting that glycogen metabolism may be strongly inhibited under exposure to E_2 and, unexpectedly, slightly inhibited by P_4 treatment. Thus, decreased PGM activity may be part of the mechanism by which E2 enhances insulin's stimulatory effects on glycogen storage. Such inhibition would not raise glycogen levels in the absence of increased glucose supply.

Discussion

We have measured for the first time the effect of hormones (E_2 and P_4) treatment on both the activities (V_{max}) and kinetics of the enzymes of glycolysis in a single model system (GMMe). Furthermore, it is the first time for such complete measurements in uterine cells derived from an animal with an obligate diapause phase of reproduction. The results are markedly different from other mammals *in vivo* but consistent with patterns observed previously for *in vitro* studies and GMMe [22,24]. While these hormones alone *in vitro* did not alter glycolytic flux, metabolite levels and the glucose consumption in the GMMe cells, treatment with E_2 induced a decrease in most enzyme activities, while P_4 alone induced an increase in several K_ms.

Glycolytic enzyme expression, but not activity, has been measured previously both in live mink and in cultured mink endometrial cells. GMMe cells express GAPDH and HK-1, and GAPDH mRNA levels are not changed by P_4 and E_2 treatment [22,23]. We also found GAPDH activity was unaffected by P_4 and E_2 treatment. In live mink, HK expression was shown to increase during estrus [20], whereas GMMe HK *activity* was found to be reduced after exposure to E_2. We found only one isoform of HK to be present in cytosolic enzyme extract.

Although we found that the activity of most of the glycolytic enzyme, including HK, are decreased by E_2 treatment of GMMe (Figure 1 and Table 1), in rat uteri E_2 exposure increased the activities of all enzymes except PGM [10]. There are several explanations for the unique effects of E_2 on GMMe glycolytic enzymes, in addition to transcriptional effects. It is quite likely that P_4 and E_2 act in coordination with other hormones while regulating glycolytic enzymes *in vivo*. Insulin is required for stimulation of *in vitro* glycogen synthesis by E_2 [22]. Thus, insulin, and possibly other hormones, may also be required to attain the stimulatory effects of E_2 observed for rat glycolysis.

Regulation of glycolytic enzymes in mink may also be distinct from that of other organisms. Several enzymes within glycolysis are regulated by distinct types of post-translational modifications. For instance, phosphorylation fine-tunes the metabolism network and receives signals from upstream hormones. Thus, enzymes in mink uterine tissue and GMMe cells may exhibit a distinct profile of modifications compared with those in tissues. It is also possible that there

is variation in post-translational modifications and glycolytic enzyme isoforms between mink and other mammals such as rats.

We also measured for the first time the K_ms of glycolytic enzymes in immortalized endometrial cells. Pyruvate kinase K_ms were nearly identical to those measured in mink liver [24] ($Km_{PEP} = 0.209$ vs. 0.230 mM GMMe; $Km_{ADP} =$ 0.380 vs. 0.230 mM, liver vs. GMMe, respectively). For enolase, Km_{2PG} was lower in mink than in *Rattus norvegicus*, whereas for LDH Km_{Lac} was substantially higher in mink (Table 1). For PGM, Km_{G1P} increased more than 40-fold with exposure to E_2 (26 ± 15 to 1200 ± 346 μM) (Table 1). Thus, PGM velocity would be decreased by 89% under these conditions. This suggested that either the expression of a low-affinity PGM isoform is induced by E_2 or post-translational modification, essentially preventing G1P from being converted into G6P. This is consistent with the fact that E_2 blocks glycogen mobilization in mink uterine epithelial cells [22]. Because E_2 is unable to stimulate glycogen synthesis in GMMe cells in the absence of insulin [22], the inhibition of PGM by E_2 may be permissive rather than sufficient for glycogen synthesis.

If the decreases in glycolytic enzyme activities are priming glucose metabolism for regulation by insulin, alone P_4 and E_2 would not necessarily have any effects on the glycolytic flux. We did not observe any significant changes in overall lactate production for GMMe cells (Figure 2). While E_2 has been shown, in a few studies in rats, to increase uterine glycolytic flux [13,32,33], these studies have been of recently harvested tissue, putatively after exposure to insulin. This is congruent with recent studies that found an important role for insulin in mediating the effects of uterine hormones [22,23]. E_2 has been previously shown to work in coordination with insulin on uterine carbohydrate metabolism. For instance, E_2 increases insulin receptors over two-fold in the uteri of ovariectomized rats [34].

Similarly, no significant changes were observed for glucose transport in GMMe. In rat uterine tissues, glucose uptake and consumption were increased by E_2 exposure *in vivo* [32,33]. P_4 increased glucose transporter expression in sheep [34] and mice [35] where E_2 also decreased expression. However, the levels of insulin *in vivo* were not controlled and were presumably non-zero. Thus, E_2 and P_4 *in vivo* were likely acting in concert with physiological levels of insulin or insulin-like growth factor (IGF1) to affect transport. There is currently no evidence that E_2 and P_4 regulate glucose transport without insulin, as glucose transporters in human cells *in vitro* were not directly regulated by E_2 or P_4 [36].

The inability of E_2 and P_4 treatment to affect glucose usage in GMMe, despite substantial changes in enzyme activities, supports the growing evidence that these ovarian hormones are not able to act independently to affect uterine metabolism and development [22,23]. Studies performed before the identification of IGF1 asserted that uterine glycogen synthesis was independent of insulin [35]. This dogma needs reassessment. Hormones such as insulin and IGF1 appear to be needed to couple reproduction to energy metabolism across a range of organisms and their tissues [36,37]. If this mechanism extends to humans, the insulin resistance that underlies metabolic syndrome and associated female infertility (reviewed [38]) may be connected to the inability of insulin to affect the ability of ovarian hormones (E_2 and P_4) to properly change carbohydrate use in uterine tissues.

Finally, although kinetic analysis and flux measurement provide insight into GMMe glycolysis, there is not a simple relationship between changes in enzyme kinetics, fluxand the behavior of a system. Recent studies have demonstrated that the kinetics and kinetic mechanisms of enzymes measured in physiological conditions can be used to create effective models of metabolism [39,40]. Thus, our data could be used to construct a computational model for GMMe similar to that of HeLa [29,30], which demonstrated an effective approach to integrating *in vitro* data to construct a quantitative model of nutrient metabolism using COPASI software [41]. With such a model, we could develop hypotheses for future experiments. For instance, we could predict the effects of changes in blood glucose or determine how hormones affect which enzymes exert the most control over the carbohydrate allocation.

Competing Interests

The authors declare that there are no competing interests associated with the manuscript.

Funding

This work was supported by the Institutional Development Award (IDeA) from the National Institute of General Medical Sciences of the National Institutes of Health [grant number #P20GM103408]; and Alan Crews & the NNU Science, Math, and Engineering Associates for equipment funding. Its contents are solely the responsibility of the authors and do not necessarily represent the official views of NIH.

Author Contribution

Hayden Holmlund: Wrote the main draft of the manuscript and carried out the majority of the enzyme kinetics measurements. Álvaro Marín-Hernández: Trained the researchers in the techniques, edited the manuscript, and provided supervision. Jennifer R. Chase: Edited the manuscript, was awarded the funding, supervised and designed the study, and worked with the GMMe cells.

Acknowledgements

The authors wish to thank Ayokunle Hodonu, Andrew Holston, Angelique Yang, Abigail Haas, Lauren Gould, Brittany Sanchez, Tracey Cook, Hunter Bain, Stephen Christensen, and Katelyn Heckathorn for technical assistance.

Abbreviations

ADP, adenosine diphosphate; ALDO, aldolase (E.C 4.1.2.13); ATP, adenosine triphosphate; BCA, bicinchoninic acid; DHAP, dihydroxyacetone phosphate; DMSO, dimethyl sulfoxide; ENO, enolase (E.C. 4.2.1.11); E_2, 17-β-estradiol; F1,6BP, fructose 1,6-bisphosphate; F6P, fructose 6-phosphate; GAPDH, glyceraldehyde-3-phosphate dehydrogenase; G1P, glucose 1-phosphate; G3P, glyceraldehyde 3-phosphate; G6P, glucose 6-phosphate; G6PDH, glucose-6-phosphate dehydrogenase (E.C. 1.1.1.49); HK, hexokinase (E.C. 2.7.1.1); HPI, phosphohexose isomerase (E.C. 5.3.1.9); IGF1 , insulin-like growth factor; LDH, lactate dehydrogenase (E.C. 1.1.1.27); NAD(H), nicotinamide adenine dinucleotide; PEP, phosphoenolpyruvate; PFK-1, phosphofructokinase type I (E.C. 2.7.1.11); PGaM, phosphoglycerate mutase (E.C. 2.7.2.3); PGK, phosphoglycerate kinase (E.C. 5.4.2.1); PGM, phosphoglucomutase (E.C. 5.4.2.2); PYK, pyruvate kinase (E.C. 2.7.1.40); P_4, progesterone; TIM, triosephosphate isomerase (E.C. 5.3.1.1); 2PG, 2-phosphoglycerate; 3PG, 3-phosphoglycerate.

References

1 Wilcox, A.J. et al. (1988) Incidence of early loss of pregnancy. *N. Engl. J. Med.* **319**, 189–194, https://doi.org/10.1056/NEJM198807283190401
2 Diskin, M. and Morris, D. (2008) Embryonic and early foetal losses in cattle and other ruminants. *Reproduct. Domest. Anim.* **43**, 260–267, https://doi.org/10.1111/j.1439-0531.2008.01171.x
3 Leese, H.J. (2012) Metabolism of the preimplantation embryo: 40 years on. *Reproduction* **143**, 417–27, https://doi.org/10.1530/REP-11-0484
4 Brinster, R.L. (1965) Studies on the development of mouse embryos *in vitro*. *Reproduction* **10**, 227–240, https://doi.org/10.1530/jrf.0.0100227
5 Hempstock, J. et al. (2004) Endometrial glands as a source of nutrients, growth factors and cytokines during the first trimester of human pregnancy: a morphological and immunohistochemical study. *Reproduct. Biol. Endocrinol.* **2**, 1–14, https://doi.org/10.1186/1477-7827-2-58
6 Amoroso, E. (1952) Placentation. In *Marshall's Physiology of Reproduction* (Parkes, A.S., ed.), p. 127, Longmans Green, London
7 Pilbeam, T.E., Concannon, P.W. and Travis, H.F. (1979) The annual reproductive cycle of mink (*Mustela vison*). *J. Anim. Sci.* **48**, 578–584, https://doi.org/10.2527/jas1979.483578x
8 Demers, L.M. and Jacobs, R.D. (1973) Comparative effects of ovarian steroids on glycogen metabolism of rat, rabbit and guinea pig uterine tissue. *Proc. Soc. Exp. Biol. Med.* **143**, 1158–1163, https://doi.org/10.3181/00379727-143-37491
9 Ahmed-Sorour, H. and Bailey, C. (1981) Role of ovarian hormones in the long-term control of glucose homeostasis glycogen formation and gluconeogenesis. *Ann. Nutr. Metab.* **25**, 208–212, https://doi.org/10.1159/000176496
10 Carrington, L. and Bailey, C. (1985) Effects of natural and synthetic estrogens and progestins on glycogen deposition in female mice. *Horm. Res. Paediatr.* **21**, 199–203, https://doi.org/10.1159/000180045
11 Rose, J. et al. (2011) The effects of estradiol and catecholestrogens on uterine glycogen metabolism in mink (Neovison vison). *Theriogenology* **75**, 857–866, https://doi.org/10.1016/j.theriogenology.2010.10.028
12 Chase, C. et al. (1992) In vitro metabolism of glucose by bovine reproductive tissues obtained during the estrous cycle and after calving. *J. Anim. Sci.* **70**, 1496–1508, https://doi.org/10.2527/1992.7051496x
13 Shinkarenko, L., Kaye, A.M. and Degani, H. (1994) 13C NMR kinetic studies of the rapid stimulation of glucose metabolism by estrogen in immature rat uterus. *NMR Biomed.* **7**, 209–217, https://doi.org/10.1002/nbm.1940070503
14 Reiss, N.A. (1988) Ontogeny and estrogen responsiveness of creatine kinase and glycolytic enzymes in brain and uterus of rat. *Neurosci. Lett.* **84**, 197–202, https://doi.org/10.1016/0304-3940(88)90407-7
15 de Asua, L.J., Rozengurt, E. and Carminatti, H. (1968) Estradiol induction of pyruvate kinase in the rat uterus. *Biochim. Biophys. Acta Gen. Subjects* **170**, 254–262, https://doi.org/10.1016/0304-4165(68)90005-6
16 Singhal, R.L. and Valadares, J. (1970) Estrogenic regulation of uterine pyruvate kinase. *Am. J. Physiol. Legacy Content* **218**, 321–327, https://doi.org/10.1152/ajplegacy.1970.218.2.321
17 Murdoch, B. and O'Shea, T. (1978) Activity of enzymes in the mucosal tissues and rinsings of the reproductive tract of the naturally cyclic ewe. *Aust. J. Biol. Sci.* **31**, 345–354, https://doi.org/10.1071/BI9780345
18 Murdoch, R. and White, I. (1968) Activity of enzymes in the endometrium, caruncles, and uterine rinsings of progestogen-treated and naturally cycling ewes. *Aust. J. Biol. Sci.* **21**, 123–132, https://doi.org/10.1071/BI9680123
19 Bowman, K. and Rose, J. (2017) Estradiol stimulates glycogen synthesis whereas progesterone promotes glycogen catabolism in the uterus of the American mink (*Neovison vison*). *Anim. Sci. J.* **88**, 45–54, https://doi.org/10.1111/asj.12564

20 Dean, M. et al. (2014) Uterine glycogen metabolism in mink during estrus, embryonic diapause and pregnancy. *J. Reprod. Dev.* **60**, 438–446, https://doi.org/10.1262/jrd.2014-013
21 Moreau, G.M. et al. (1995) Development of immortalized endometrial epithelial and stromal cell lines from the mink (*Mustela vison*) uterus and their effects on the survival *in vitro* of mink blastocysts in obligate diapause. *Biol. Reprod.* **53**, 511–518, https://doi.org/10.1095/biolreprod53.3.511
22 Dean, M. and Rose, J. (2018) Activation of the IGF1 receptor stimulates glycogen synthesis by mink uterine epithelial cells. *Mol. Reprod. Dev.* **85**, 449–458, https://doi.org/10.1002/mrd.22981
23 Hodonu, A. et al. (2019) Glycogen metabolism in mink uterine epithelial cells and its regulation by estradiol, progesterone and insulin. *Theriogenology* **130**, 62–70, https://doi.org/10.1016/j.theriogenology.2019.02.023
24 Sorensen, P., Petersen, I. and Sand, O. (1995) Activities of carbohydrate and amino acid metabolizing enzymes from liver of mink (*Mustela vison*) and preliminary observations on steady state kinetics of the enzymes. *Comp. Biochem. Physiol. B Biochem. Mol. Biol.* **112**, 59–64, https://doi.org/10.1016/0305-0491(95)00056-E
25 Lagerkvist, G. et al. (1992) Profiles of oestradiol-17β and progesterone and follicular development during the reproductive season in mink (*Mustela vison*). *Reproduction* **94**, 11–21, https://doi.org/10.1530/jrf.0.0940011
26 Hynes, A.M. and Rouvinen-Watt, K. (2007) Monitoring blood glucose levels in female mink during the reproductive cycle: 1. Prevention of hyperglycemia during the nursing period. *Can. J. Vet. Res.* **71**, 241
27 Wamberg, S. et al. (1992) Nursing sickness in lactating mink (*Mustela vison*). II. Pathophysiology and changes in body fluid composition. *Can. J. Vet. Res.* **56**, 95
28 Smith, P.K. et al. (1985) Measurement of protein using bicinchoninic acid. *Anal. Biochem.* **150**, 76–85, https://doi.org/10.1016/0003-2697(85)90442-7
29 Marín-Hernández, A. et al. (2014) Modeling cancer glycolysis under hypoglycemia, and the role played by the differential expression of glycolytic isoforms. *FEBS J.* **281**, 3325–3345, https://doi.org/10.1111/febs.12864
30 Rodríguez-Enríquez, S., Torres-Márquez, M.E. and Moreno-Sánchez, R. (2000) Substrate oxidation and ATP supply in AS-30D hepatoma cells. *Arch. Biochem. Biophys.* **375**, 21–30, https://doi.org/10.1006/abbi.1999.1582
31 Marín-Hernández, A. et al. (2011) Modeling cancer glycolysis. *Biochim. Biophys. Acta Bioenerg.* **1807**, 755–767, https://doi.org/10.1016/j.bbabio.2010.11.006
32 Lea, M.A., Singhal, R.L. and Valadares, J. (1970) Metabolic control mechanisms in mammalian systems-VI: estrogenic control of uterine lactate and α-glycerophosphate production in ovariectomized rats. *Biochem. Pharmacol.* **19**, 113–124, https://doi.org/10.1016/0006-2952(70)90332-1
33 Roberts, S. and Szego, C.M. (1953) The influence of steroids on uterine respiration and glycolysis. *J. Biol. Chem.* **201**, 21–30
34 Koricanac, G. et al. (2008) Insulin signaling in the liver and uterus of ovariectomized rats treated with estradiol. *J. Steroid Biochem. Mol. Biol.* **108**, 109–116, https://doi.org/10.1016/j.jsbmb.2007.06.001
35 Swigart, R.H. et al. (1962) The insulin independence of uterine glycogen in the rat. *Endocrinology* **70**, 600–602, https://doi.org/10.1210/endo-70-4-600
36 Burks, D.J. et al. (2000) IRS-2 pathways integrate female reproduction and energy homeostasis. *Nature* **407**, 377, https://doi.org/10.1038/35030105
37 Bell, A.W. and Bauman, D.E. (1997) Adaptations of glucose metabolism during pregnancy and lactation. *J. Mammary Gland Biol. Neoplasia* **2**, 265–278, https://doi.org/10.1023/A:1026336505343
38 Al Awlaqi, A., Alkhayat, K. and Hammadeh, M.E. (2016) Metabolic syndrome and infertility in women. *Int. J. Womens Health Reprod. Sci.* **4**, 89–95, https://doi.org/10.15296/ijwhr.2016.23
39 van Eunen, K. et al. (2012) Testing biochemistry revisited: how *in vivo* metabolism can be understood from *in vitro* enzyme kinetics. *PLoS Comput. Biol.* **8**, e1002483, https://doi.org/10.1371/journal.pcbi.1002483
40 Mulquiney, P.J. and Kuchel, P.W. (1999) Model of 2,3-bisphosphoglycerate metabolism in the human erythrocyte based on detailed enzyme kinetic equations1: equations and parameter refinement. *Biochem. J.* **342**, 581–596, https://doi.org/10.1042/bj3420581
41 Mendes, P., Hoops, S., Sahle, S., Gauges, R., Dada, J. and Kummer, U. (2009) Computational modeling of biochemical networks using COPASI. In *Systems Biology. Methods in Molecular Biology (Methods and Protocols)* (Maly, I., ed.), vol. 500, Humana Press